Optimization Modeling of the Hybrid Antenna Array for the DoA Estimation

Somayeh Komeylian

Abstract—The direction of arrival (DoA) estimation is the crucial aspect of the radar technologies for detecting and dividing several signal sources. In this scenario, the antenna array output modeling involves numerous parameters including noise samples, signal waveform, signal directions, signal number, and signal to noise ratio (SNR), and thereby the methods of the DoA estimation rely heavily on the generalization characteristic for establishing a large number of the training data sets. Hence, we have analogously represented the two different optimization models of the DoA estimation; (1) the implementation of the decision directed acyclic graph (DDAG) for the multiclass least-squares support vector machine (LS-SVM), and (2) the optimization method of the deep neural network (DNN) radial basis function (RBF). We have rigorously verified that the LS-SVM DDAG algorithm is capable of accurately classifying DoAs for the three classes. However, the accuracy and robustness of the DoA estimation are still highly sensitive to technological imperfections of the antenna arrays such as non-ideal array design and manufacture, array implementation, mutual coupling effect, and background radiation and thereby the method may fail in representing high precision for the DoA estimation. Therefore, this work has a further contribution on developing the DNN-RBF model for the DoA estimation for overcoming the limitations of the non-parametric and data-driven methods in terms of array imperfection and generalization. The numerical results of implementing the DNN-RBF model have confirmed the better performance of the DoA estimation compared with the LS-SVM algorithm. Consequently, we have analogously evaluated the performance of utilizing the two aforementioned optimization methods for the DoA estimation using the concept of the mean squared error (MSE).

Keywords—DoA estimation, adaptive antenna array, Deep Neural Network, LS-SVM optimization model, radial basis function, MSE.

I. INTRODUCTION

THE DoA estimation has recently received an increasing demand for its potential use in a variety of applications such as wireless communications, navigation, tracking of various targets, rescue and other emergency assistance devices, radio astronomy, sonar, and radars. In the radar applications, the DoA estimation is performed for the accurate localization of targets. In the applications of wireless communications, the DoA estimation provides the spatial diversity for the receiver in the multi-user technologies. The DoA estimation is very much affected by the parameters of the signal source and the propagation medium.

Of various interesting and exciting solutions in the field of the DoA estimation, this work has a major contribution on

Somayeh Komeylian is with the Electrical Engineering Department, Ryerson University, Toronto, Canada (e-mail: skomeylian@ryerson.ca).

developing the array signal processing technique for the DoA estimation. Array signal processing allows processing and analyzing signals received by the antenna array for achieving the objectives of strengthening signals in the direction of interest, eradicating interference signals, and estimating some of signal parameters precisely. In this scenario, array signal processing algorithms ensure better resolution performance of signal reception as well as better performance in steering the mainbeam in the direction of interest and in suppressing interference signals.

The conventional algorithms failed to recognize the distinction between signals rejected by the two scenarios of destructive combination of correlated signals and spatial nulls under jamming circumstances and multipath propagation. Neural network optimization methods have potential applications in modeling and forecasting for unseen scenarios [5], [6]. However, some practical challenges in performing the neural network optimization methods, including local minima and overfitting, have been reported by various research groups [7]-[9]. Then, based on Structural Risk Minimization (SRM) principle [7]-[10], SVM optimization methods were developed by Platt et al. [10], for overcoming the aforementioned limitations [7]-[10]. The main advantage of the SVM optimization methods consists of employing global optimum rather than a local optimum. Therefore, a drastic reduction of overfitting is achievable by choosing the maximum margin hyperplane in the feature space. However, the practical implications of performing the SVM optimization methods reside in the three main disadvantages; (1) the involved problems require solving a quadratic programing (QP) problem with a very low speed, especially, for a large-scale practical problem, (2) upper bound parameter and kernel parameters are not appropriately optimized in the SVM model, (3) relevant input features are not efficiently estimated. In this scenario, a feasible way for enhancing generalization performance and decreasing computational cost as well as for fostering degree of the accuracy in the DoA estimation consists of exploiting the LS-SVM optimization method.

The LS-SVM optimization methods rely on data-driven computations without having any pre-assumption about antenna array geometries and antenna array calibration. However, under the aforementioned conditions, these methods may fail in representing high precision for the DoA estimation. Deep learning-based methods allow reconstructing complex propagation models, relying on training data sets, and then, estimating source directions and locations. The main advantage of the DNNs over the different available NNs resides in the fact that they represent a very high accurate and

World Academy of Science, Engineering and Technology
International Journal of Electronics and Communication Engineering
Vol:15, No:2, 2021

robust performance, due to extra neuron layers added to their structures. Hence, this study has a major contribution for exploiting the DNN-RBF modeling of the DoA estimation. In this scenario, we have employed the gradient descent method for the supervised learning of the DNN-RBF method to minimize the MSE. In order to further boost the functionality of the 3D DoA estimation in terms of the resolution and accuracy, in addition to exploiting optimization modeling, we have proposed the hybrid antenna array geometry. Indeed, the mainbeam characteristics and beam scanning capability of the adaptive antenna array are very much affected by the array geometry. The geometry of the hybrid antenna array comprises of cylindrical subarrays, as shown in Fig. 1. Each cylindrical subarray is composed of two concentric circular subarrays positioned upon each other. The suggested configuration in Fig. 1 provides major advantages including a reduction in the number of elements, and size, which is comparable to that obtainable with an ideal case of spherical array [11].
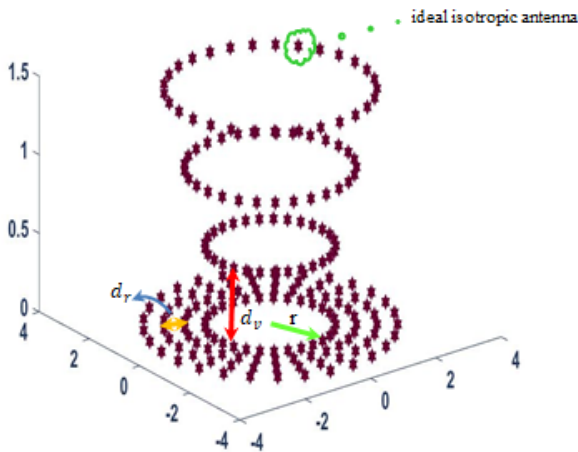

Fig. 1 The geometry of the hybrid antenna array comprising of cylindrical subarrays. Each cylindrical subarray is composed of two concentric circular subarrays positioned upon each other [14]. The 3D configuration of the proposed antenna array plotted with MATLAB codes. The design parameters of the hybrid antenna array are assigned in details in Table I. It is assumed that the source of each array element is an ideal isotropic antenna

TABLE I
DESIGN PARAMETERS OF THE PROPOSED ANTENNA ARRAY

Parameters	Definition	Value
N	Number of elements of any circular loop	N = 20
Q	Number of elements of any cylinder	Q = 40
M	Total number of cylinders in the proposed array	M = 3
P	Number of circular loops in the cylinder	P = 2
d_v	Vertical spacing between two consecutive circular loops	$d_v = 0.5\lambda$
d_r	Horizontal spacing between two consecutive circular loops	$d_r = 0.5\lambda$
φ, θ	Maximum scanning angles	$\varphi = 45°, \theta = 45°$

II. A BRIEF REVIEW OF THE RBF NEURAL NETWORK MODELING

The discussion in this section focused on reviewing the NN-RBF optimization method. The neural network model can adjust it to the data without having a priori knowledge about the form of the underlying function or distribution which is being estimated. Indeed, the data-driven neural network refers to the self-adaptive modeling. Since the involved problems of the neural network consist of some kind of non-linear optimizations, the neural network modeling is an excellent candidate for estimating complex real-world relationships.

Based on the universal approximation theorem, the neural network model can estimate the underlying function with any arbitrary accuracy. Owing to the neural network is capable of estimating posterior probabilities; therefore it represents the basis for establishing classification rule and performing statistical analysis [3]-[5].

The supervised learning algorithms are designed to learn by the training set, in which the correct values of outputs are paired with the correct values of outputs in the following form [12]:

$$\tau = \{\boldsymbol{x}_i, \hat{y}_i^c\}_{i=1,c=1}^{i=n,c=C} \quad (1)$$

The training set of the NN only specifies $\hat{y}_i$ which involves the correct value of y_i and a small amount of unknown noise.

The training procedure in the hidden layer is unsupervised learning based on identifying commonalities. In other words, the RBF activation function in each hidden unit estimates the Euclidean distance between the input vector and the center of that unit using the Gaussian function [12].

Estimating values for the weights of the NN can happen during the training procedure between the hidden layers and the output layer, which refers to the supervised learning. Moreover, the modification of the center of the activation function should be fulfilled during the training procedure. In this scenario, the adjustment of the weights and the center of activation functions are performed using the gradient descent method for minimizing non-linear the sum-squared-error.

Mathematical Formulas of the Training Procedure:

a) Unsupervised Learning: The model of f is expressed as a linear combination of a set of the M fixed basis functions,

$$f(\boldsymbol{x}_i) = \sum_{j=1}^{M} \omega_{ij} h_{ij}(\boldsymbol{x}_i) \quad (2)$$

where M refers to the number of neurons. ω_{ij} is the weights of neurons in the linear output. $h_{ij}(\boldsymbol{x}_i)$ reflects the basis functions in the hidden units.

$$h_{ij}(\boldsymbol{x}_i) = \varphi\|\boldsymbol{x}_i - \boldsymbol{c}_j\| \quad (3)$$

where $\boldsymbol{c}_j$ refers to the center vector of neurons.

$$\varphi(x) = a * \exp\left(-\frac{(x-\mu)^2}{2*\sigma_i^2}\right) \quad (4)$$

World Academy of Science, Engineering and Technology
International Journal of Electronics and Communication Engineering
Vol:15, No:2, 2021

where a and μ indicate the height of the curve center and the horizontal position of the center of the curve peak, respectively. In addition, σ denotes the standard deviation.

b) Supervised Learning: The least squares recipe is to minimize the sum squared error in the output in the formula:

$$S = \sum_{i=1}^{P} (\hat{y}_i - f(x_i))^2 \qquad (5)$$

The gradient descent has been employed for minimizing the sum squared error in [3]-[6]:

$$\omega_{ij}(\text{new}) = \omega_{ij}(\text{old}) - \eta \frac{\partial E}{\partial \omega_{ij}} \qquad (6)$$

where η refers to the learning rate and E is defined as:

$$E(\omega_{ij}) = \frac{1}{P} S(\omega_{ij}) \qquad (7)$$
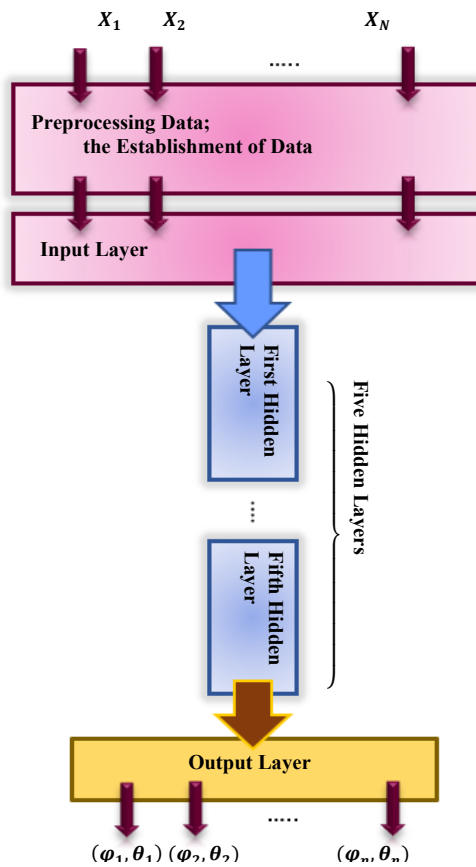

Fig. 2 System structure of implementing the RBF-DNN model for the DoA estimation. The results of this algorithm have been obtained assuming the five layers are arranged in series

III. A BRIEF REVIEW OF THE LS-SVM MODELING

Suykens et al. [8], [12] introduced LS-SVM algorithm, which is defined by the following equations:
Find

$$f(x) = \text{sign}(\omega\ \Gamma(x_i) + b) \qquad (8)$$

- By minimizing

$$\mathcal{L}_{LS}(\omega, \varphi) = \frac{1}{2}\|\omega\|^2 + \frac{1}{2}\gamma \sum_{i=1}^{n} \varphi_i^2 \qquad (9)$$

- Subject to constraints:

$$y_i[\omega^T \Gamma(x_i) + b] \geq 1 - \varphi_i \quad \text{for } i=1, 2,\ldots,n \qquad (10)$$

where the regularization parameter of γ is applied to the data in the feature space for regulating the complexity of the machine learning model [8], [12]. Moreover, the equation of $w.\Gamma(x_i) + b = 0$ refers to the hyperplane definition with the largest margin. Furthermore, w and b represent the weight vector perpendicular to the separating hyperplane and the bias value for shifting the hyperplane parallel to itself, respectively [8], [12].

It is worth mentioning that the discriminative LS-SVM models exploit the exponential kernel transformation, $\Gamma(x_i)$, for mapping the input data in the input space into the data in higher dimensional feature space. Indeed, kernel functions in machine learning algorithms, as a nonlinear mapping, generate the scalar dot products of the input/output pairs in the feature space. Since different kernel functions generate different SVMs, thereby, the performance of each LS-SVM is very much affected by choosing an appropriate kernel function. Hence, the non-linear mapping function of $\Gamma(x_i)$ is associated to the kernel of $\mathbb{K}(x.x_i)$ in the following form [8], [12]:

$$\Gamma(x).\Gamma(x_i) = \mathbb{K}(x.x_i) \qquad (11)$$

There is a growing literature of presenting the LS-SVM optimization methods in the various applications; thereby, we have concisely reviewed the theoretical backgrounds of the one-vs-one DDAG LS-SVM modeling of the adaptive antenna array for the DoA estimation in the following procedures;

A. Preprocessing Procedure

A) Produce the D×N training signal vector for the number of C classes of LS-SVM model. It is worth mentioning that the training signal is not necessarily a vector.

B) Produce C number of the sample covariance matrixes, U, in which M number of samples are from the D×N training signal data. Eigen decomposition or subspace tracking technique allows achieving the desired vectors of w, which are eigenvectors of the covariance matrix of the input data signal. In this scenario, the maximum vectors of w are associated with the largest eigenvalues of the covariance matrix.

C) Calculate the eigenvectors, S, for each of the C sample covariance matrices for the aforementioned purpose in the part B.

D) Calculate the projection vectors of U.S.

E) Store the projection vectors for the training step and the eigenvectors for the testing step.

1. Training procedure: Modeling

1.1. Using the decision function and C projection vectors train

World Academy of Science, Engineering and Technology
International Journal of Electronics and Communication Engineering
Vol:15, No:2, 2021

the $\frac{C(C-1)}{2}$ nodes in the one-vs-one LS-SVM algorithm.

1.2. Calculate the LS-SVM variables, α_i and b, using the decision function, which refers to the separating hyperplane in each of DDAG nodes.

2. Testing procedure: Labeling

2.1. The two sets of projection coefficients (D× 1 projection vectors) at each of the ith/jth node of the DDAG are obtained by the products of the desired eigenvector covariance matrix and the ith and jth eigenvectors from the training procedure.

2.2. The new set of projection vectors are tested using the ith/ jth hyperplane, which means performing the two separate LS-SVM testing cycles; one cycle is for the projection vector from the ith vector and another cycle is for the projection vector from the jth vector.

$$\hat{y}_i = \omega^T \Gamma(x_i) + b \tag{12}$$

2.3. Compute the mean values of the two LS-SVM output vectors or labels. Then, compare the recent mean values with the label definition at the node and choose the mean value with the smallest hit count. The hit count of the H_i is expressed by:

$$\mathbf{H}_i = \begin{cases} 1 & |\hat{y}_i - y_i| \le \varepsilon \\ 0 & \text{Otherwise} \end{cases} \tag{13}$$

$\hat{y}_i$ and y_i refer to the predicted and observed (or seen) values, respectively. The value of ε denotes the difference between observed and predicted values.

2.4. Repeat the same procedure for the next node of the DDAG path and determine the last DoA label.

3. Error Control: The Error control procedure indeed provides a merit for classifying the labels into either an accurate DoA estimate, or noise. Furthermore, the DDAG path is evaluated by the obtained MSE values in the error control procedure [8], [12]. The validation in this step includes controlling the both empirical and theoretical MSEs and misclassification and gross errors [8], [12].
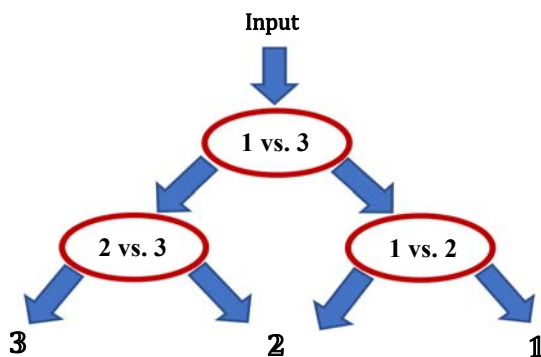

Fig. 3 Three class DDAG for one-vs-one multiclass LS-SVM for the DOA estimation

During the training procedure, the classification problems

try to assign previously unseen patterns to their respective classes using the previous training set input-output pairs of each class. Therefore, the output of the learning algorithm consists of one of the discrete set of classes instead of the value of a continuous function of a non-parametric regression problem. Values of the training set outputs, whose numbers are identical to the number of classes, consist of the vectors of length.

After training procedure, the supervised learning algorithm considers the new inputs and then it determines the label of the new outputs based on the prior training data.

IV. THE DoA ESTIMATION

We consider the number of K independently-narrowband plane waves propagating in the linear and isotropic medium, impinging on the M elements of the given antenna array. The kth narrowband waveform is supposed to be $S_k(t)$ for k = 1, 2, …, K, assuming M>K. The array outputs are calculated at the samples of N uniquely-spaced time instants, $t_1, t_2, …., t_N$, for obtaining snapshots of $X(t) = [x(t_1)\ x(t_2)\dots x(t_N)]$. Hence, the antenna array outputs can be expanded in terms of the beam steering vector of the antenna array of $a(\varphi_k, \theta_k)$ towards the direction of (φ_k, θ_k) [1]-[12] and the zero-mean Gaussian noise vector of $v_n(t)$ [1]-[12] in the following expression,

$$x(t_n) = \sum_{k=1}^{K} a(\varphi_k, \theta_k)S_k(t_n) + v(t_n) + i(t_n) \text{ for n} = 1, 2,…,N \tag{14}$$

The elements of the antenna array are capable of performing a mapping from the DoA space, $\{\Theta = [(\varphi_1, \theta_1), (\varphi_2, \theta_2), …, (\varphi_k, \theta_k)]^T\}$, to the space of the antenna array, $\{X(t) = [x(t_1)\ x(t_2)\dots x(t_N)]^T\}$; $G: R^K \to C^M$. However, the NN modeling is exploited to perform the inverse mapping; $G: C^K \to R^M$, Fig. 4.

The received spatial correlation matrix (or the covariance matrix) of **R** is expressed by the following form [1]-[12]:

$$\mathbf{R} = \text{E}\{\mathbf{X}(t)\mathbf{X}^H(t)\} = \mathbf{A}\text{E}(\mathbf{S}(t)\ \mathbf{S}^H(t))\mathbf{A}^H + \text{E}(\mathbf{V}(t)\ \mathbf{V}^H(t)) \tag{15}$$

Before implementing any optimization method, we aim at establishing the data using the minimum variance distortionless response (MVDR) beamformer [13]. Indeed, the adaptive beamforming algorithm allows achieving the high performance of the antenna array in terms of robustness against the imperfect, incomplete and erroneous information about the antenna array, the signal source, and propagation media.

The primary goal of the MVDR beamforming technique is to minimize the signal to interference noise ratio (SINR) expressed by [13]:

$$\text{SINR} \triangleq \frac{\text{E}\left(|w^H S|^2\right)}{\text{E}\left(|w^H(n+k)|^2\right)} = \frac{\sigma_s^2 |w^H a(\varphi_k, \theta_k)|^2}{w^H R_{n+k} w} \tag{16}$$

in which $\sigma_s^2 \triangleq E[|s(t_n)|^2]$ refers to the power of the signal of

World Academy of Science, Engineering and Technology
International Journal of Electronics and Communication Engineering
Vol:15, No:2, 2021

interest. The $M \times M$ covariance matrix of the interference-plus-noise of R_{n+k} is defined in:

$$R_{n+k} \triangleq E[(i(t_n) + V(t_n))((i(t_n) + V(t_n))^H] \quad (17)$$
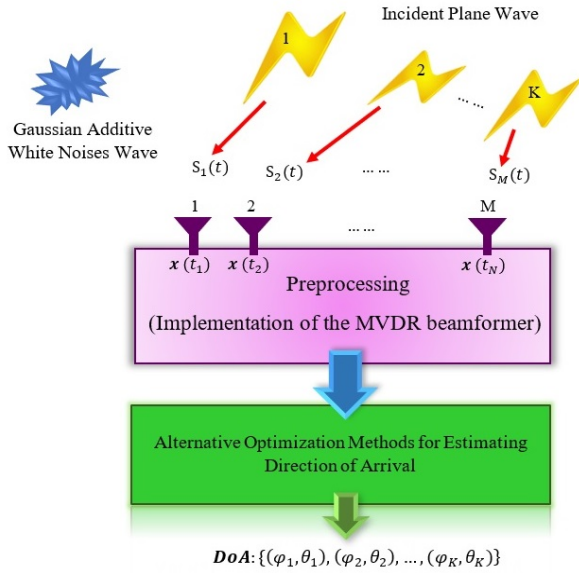

Fig. 4 System structure of the DoA estimation

Hence, the minimum SINR is achieved by the MVDR beamforming technique when the following condition is satisfied:

$$\min_w \boldsymbol{w}^H \boldsymbol{R}_{n+k} \boldsymbol{w} \quad (18)$$

Subjected to $\boldsymbol{w}^H \boldsymbol{a}(\varphi_k, \theta_k) = 1$ \quad (19)

Hence, the solution of the MVDR beamforming technique is expressed,

$$\boldsymbol{w}_{(MVDR)} = \alpha \boldsymbol{R}_{-n+k}^{-1} \boldsymbol{a}(\varphi_k, \theta_k) \quad (20)$$

The normalized constant of α in (22), which does not have any effect on the SINR and thereby it can be omitted, is given,

$$\alpha = \frac{1}{a^H(\varphi_k, \theta_k) R_{-n+k}^{-1} a(\varphi_k, \theta_k)} \quad (21)$$

Fig. 5 has efficiently demonstrated the simulation results of deploying the LS-SVM optimization method and the proposed DNN-RBF optimization model for the proposed geometry of the hybrid antenna array for the DoA estimation at the frequency of 10 GHz. Since the simulation results have verified that Fig. 5 (c) has the narrowest picks, therefore the proposed DNN-RBF model allows achieving better performance in steering mainbeam as well as high-resolution capability in comparison with the LS-SVM model. However, this increased spatial spectral resolution does not always convey to more accurate DoA estimation. Therefore, in the

following, we have analogously simulated the MSEs of the DoA estimation of the two aforementioned models for the hybrid antenna array in Fig. 1. Indeed, the accuracy and reliability of the two different models have been verified and compared using the concept of the MSEs in Fig. 6. The results of the proposed DNN-RBF model are about 10^3 times more accurate and robust than the LS-SVM optimization methods in the DoA estimation.
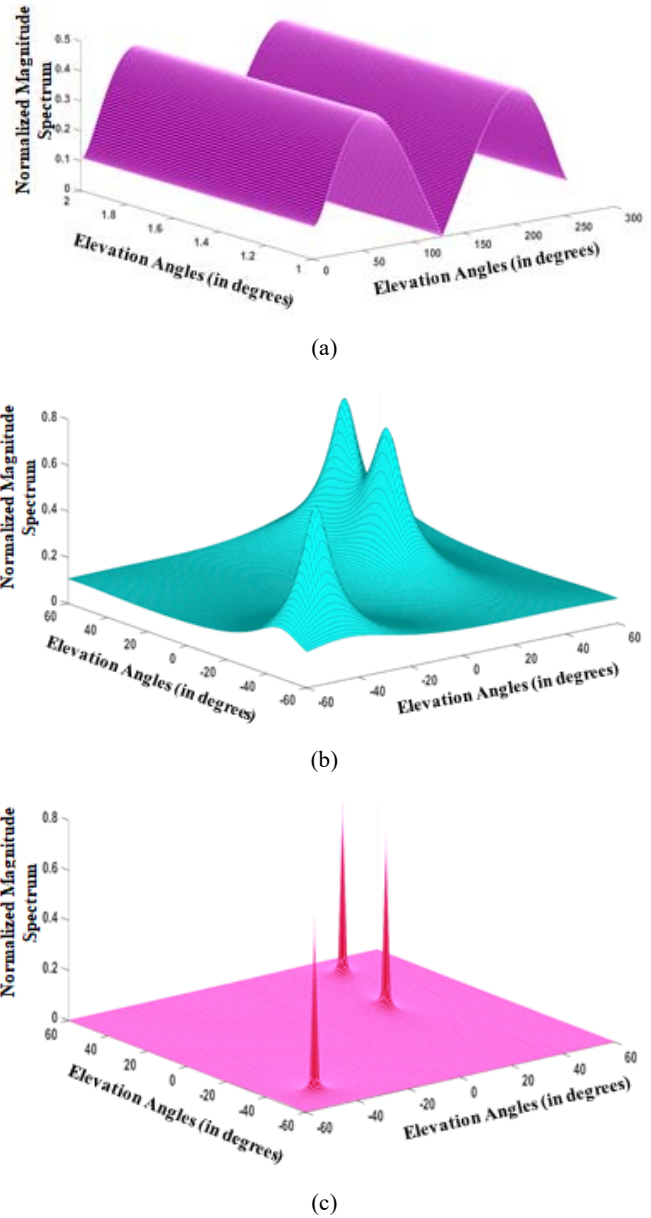

(a)

(b)

(c)

Fig. 5 Variation of normalized magnitude of DoAs at the frequency of 10 GHz using the hybrid antenna array consistent with Fig. 1, and (a) without performing any optimization method, (b) with performing the LS-SVM optimization method with three classes, and (c) with performing the DNN-RBF optimization method with the 5 hidden layers and 49 neurons and three classes

World Academy of Science, Engineering and Technology
International Journal of Electronics and Communication Engineering
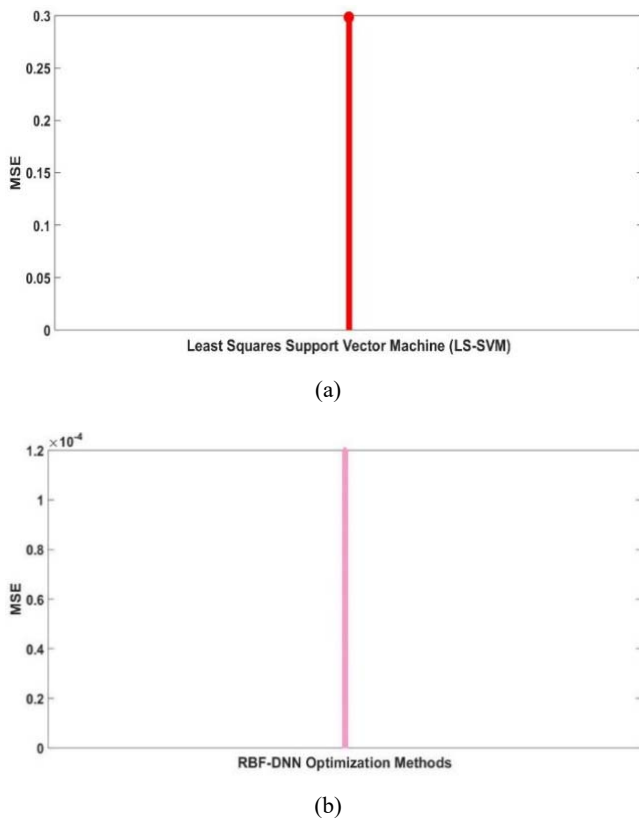Vol:15, No:2, 2021

(a)

(b)

Fig. 6 Variation of MSEs of the DoA estimation by implementing the two different optimization methods for the hybrid antenna array in Fig. 1; (a) LS-SVM optimization methods, and (b) RBF-DNN optimization methods

V. CONCLUSION

To conclude, we have rigorously implemented the two optimization methods, the DNN-RBF and the LS-SVM, for the hybrid antenna array for the DoA estimation. Analogously, simulation results have been verified that the DNN-RBF optimization methods show better performance in terms of steering the mainbeam and thereby enhancing the resolution compared with the LS-SVM optimization methods. Furthermore, the high accuracy and robustness of deploying the DNN-RBF optimization methods for the hybrid antenna array have been efficiently validated and verified in analogous to the LS-SVM optimization methods. In this scenario, simulation results on the MSEs have been represented that the proposed DNN-RBF optimization methods enable estimating DoA with 10^3 times more accurate or precise than the LS-SVM optimization methods.

REFERENCES

[1] Bindong Gao, Fangzheng Zhang, Ermao Zhao, Daocheng Zhang, and Shilong Pan, "High-resolution phased array radar imaging by photonics-based broadband digital beamforming," Optics Express 13194 27, No. 9, 2019.
[2] Najam-Us Saqib, Imdad Khan, "A Hybrid Antenna Array Design for 3-D Direction of Arrival Estimation," PLoS ONE 10(3): e0118914. doi:10.1371/journal, March 19, 2015.
[3] Sangwook Kim, Swathi Kavuri, and Minho Lee, "Deep Network with Support Vector Machines," M. Lee et al. (Eds.): ICONIP 2013, Part I, LNCS 8226, pp. 458–465, Springer-Verlag Berlin Heidelberg 2013.
[4] Gonzalo Acuña and Millaray Curilem, "Comparison of Neural Networks and Support Vector Machine Dynamic Models for State Estimation in Semiautogenous Mills," A. Hernández Aguirre et al. (Eds.): MICAI 2009, LNAI 5845, pp. 478–487, Springer-Verlag Berlin Heidelberg 2009.
[5] Yue Wu, Hui Wang, Biaobiao Zhang, and K.-L. Du, "Using Radial Basis Function Networks for Function Approximation and Classification," International Scholarly Research Network, ISRN Applied Mathematics, Article ID 324194, 34 pages, doi:10.5402/2012/324194, 2012.
[6] JAK Suykens, J De Brabanter, L Lukas, J Vandewalle, "Neurocomputing, Weighted least squares support vector machines: robustness and sparse approximation," Elsevier, 2002.
[7] A. W. Jayawardena, D. A. K. Fernando & M. C. Zhou, "Comparison of Multilayer Perceptron and Radial Basis Function networks as tools for flood forecasting," Destructive Water: Water-Caused Natural Disasters, their Abatement and Control (Proceedings of the Conference held at Anaheim, California, June 1996). IAHS Publ. no. 239, 1997.
[8] J.A.K. Suykens, and J. Vandewalle, "Least Squares Support Vector Machine Classifiers," 1999 Kluwer Academic Publishers. Printed in the Netherlands, 1999.
[9] Marija Agatonović, Zoran Stanković, Bratislav Milovanović, and Nebojša Dončov, "DOA Estimation using Radial Basis Function Neural Networks as Uniform Circular Antenna Array Signal Processor," 2011 IEEE.
[10] Yu. B. Nechaev, I.W. Peshkov, N.A. Fortunova, "Cylindrical antenna array development and measurements for DOA-estimation applications," 2017 XI International Conference on Antenna Theory and Techniques (ICATT), 2017.
[11] Slavko RUPCIC, Vanja MANDRIC, and Drago ZAGAR, "Reduction of Sidelobes by Nonuniform Elements Spacing of a Spherical Antenna Array," Radio Engineering, Vol. 20, No. 1, April 2011.
[12] Tony van Gestel, Johan A.K. Suykens, Bart Baesens, Stijn Viaene, Jan Vanthienen, Guido Dedene, Bart de Moor and Joos Vandewalle, "Benchmarking Least Squares Support Vector Machine Classifiers," 2004 Kluwer Academic Publishers, Manufactured in The Netherlands, 2004.
[13] Soodabeh Darzi, Tiong Sieh Kiong, Mohammad Tariqul Islam, Mahamod Ismail, Salehin Kibria, and Balasem Salem, "Null Steering of Adaptive Beam forming Using Linear Constraint Minimum Variance Assisted by Particle Swarm Optimization, Dynamic Mutated Artificial Immune System, and Gravitational Search Algorithm," Hindawi Publishing Corporation, the Scientific World Journal Volume 2014, Article ID 724639, 2014.
[14] Najam-Us Saqib, Imdad Khan, "A Hybrid Antenna Array Design for 3-D Direction of Arrival Estimation," PLOS ONE | DOI:10.1371/journal. pone.0118914, 2015.